Fractal topology of hand-crumpled paper

Alexander S. Balankin, Didier Samayoa Ochoa, Israel Andrés Miguel, Julián Patiño Ortiz, and Miguel Ángel Martínez Cruz
Grupo "Mecánica Fractal," Instituto Politécnico Nacional, México D.F. 07738, México

(Received 22 March 2010; published 17 June 2010)

We study the statistical topology of folding configurations of hand folded paper balls. Specifically, we are studying the distribution of two sides of the sheet along the ball surface and the distribution of sheet fragments when the ball is cut in half. We found that patterns obtained by mapping of ball surface into unfolded flat sheet exhibit the fractal properties characterized by two fractal dimensions which are independent on the sheet size and the ball diameter. The mosaic patterns obtained by sheet reconstruction from fragments of two parts (painted in two different colors) of the ball cut in half also possess a fractal scale invariance characterized by the box fractal dimension $D_{BF}=1.68\pm0.04$, which is independent on the sheet size. Furthermore, we noted that D_{BF}, at least numerically, coincide with the universal fractal dimension of the intersection of hand folded paper ball with a plane. Some other fractal properties of folding configurations are recognized.

DOI: 10.1103/PhysRevE.81.061126 PACS number(s): 46.65.+g, 89.75.Da, 05.45.Df

Crumpled configurations of thin materials are very common in nature, ranging from the microscopic level-folded proteins [1] and nanoparticle membranes [2]—to the macroscopic level—folded paper [3,4] and fault-related geological formations [5]. In mathematics, Riemann has used a crumpled ball of paper with bookworms to explain the hidden dimensions in non-Euclidean geometry [6]. Accordingly, the mechanical and topological properties of folding configurations have attached much interest from both fundamental and applied points of view [1–11].

It was found that a set of balls folded from thin sheets of different sizes L under the same force (F=const) obeys a fractal scaling law $M\propto R^D$, where $M=\rho hL^2$ is the sheet mass, ρ is the material density, R is the ball diameter, and D is the global fractal dimension of the set [4,12]. For elastic membranes with thickness $h\ll R<L$ the global fractal dimension D is expected to be universal [13–15]. Specifically, theoretical considerations and numerical simulations suggest that a set of balls folded from the phantom membranes is characterized by $D=8/3$. For balls folded from self-avoiding elastic membranes numerical simulations performed in [13,14] lead to somewhat different universal values $D=2.3$ and $D=2.5$, respectively [16]. In the case of balls folded from elastoplastic materials, such as a paper, the ball diameter increases due to strain relaxation after the folding force is withdrawn [17]. Accordingly, the global fractal dimension of the set of balls folded from elastoplastic sheets of different sizes is found to be the material dependent [4,15,17]. Here it should be pointed out the difference between experiments with hand folded papers [4,15,17] and the numerical simulations of elastoplastic sheets folding performed in [14]. In contrast to experiments with hand folded paper, in numerical simulations [14] the stress relaxation leads to the decrease of the ball diameter under a fixed folding force. Because of restricted relaxation, the compactification of elastoplastic sheets under crumpling is less effective than in the elastic case [14]. Accordingly, the difference arises from the lack of similarity of the elasto-plastic ridge patterns [14]. On the other hand, in experiments with hand folded papers it was found that the internal structure of paper balls after strain relaxation obeys the fractal scale invariance $m\propto r^{D_l}$, where m is the mass of sheet within the box of size $r<R$ and D_l is the fractal dimension of the folding configuration, which is expected to be the material independent [4,15]. Specifically, in experiments with different kinds of paper it was found that $D_l=2.64\pm0.05$ [4]. In contrast to this, the local fractal dimension of folding configurations of predominantly plastic sheets, such as aluminum foils [18], is found to be a function of the compaction ratio $k=R/L$ [19]. This is easy to understand taking into account that $D_l=3$, when $k=k_{\min}\approx1.25(h/L)^{1/3}$, whereas $D_l<3$, if $k>k_{\min}$. Furthermore, the authors of [20] have observed a spontaneous symmetry breaking in folding configurations of randomly crumpled aluminum foils as k decreases. The fundamental differences in the folding behavior of elastic, elastoplastic, and predominantly plastic sheets were pointed out in [15].

The bending deformations of paper are energetically more favorable than stretching [11]. Topologically, in the limit $h\to0$, it is not possible to confine an unstretchable two-dimensional sheet into a small three-dimensional volume by only smooth deformations [21]. Such confinement necessarily requires singular crumpling along sharp lines and vertices [11]. In real sheets these singularities smoothen resulting in a balance between stretching and bending energies [10]. The energetically preferred configurations of crumpled thin sheets consist of mostly flat regions (facets) bounded by an almost straight folds (crumpling creases) that meet in sharp vertices (developable cones) [10–17]. Folding singularities leave the impression of crumpling network in the unfolded paper sheet [17,22,23]. It was found that the crumpling network patterns in unfolded sheets of different kinds of paper are characterized by the same box fractal dimension $D_{BN}=1.83\pm0.03$ [23]. The roughness of hand folded paper ball surfaces was studied in [17]. It was found that surfaces of crumpled balls display self-affine invariance with the universal local roughness exponent $\zeta=0.72\pm0.04$ [17], whereas the global roughness of set of balls folded from sheets of different sizes is characterized by the material dependent global roughness exponent $\alpha=2/D$ [17].

In this work we study the statistical topology of randomly folded paper balls. Specifically, we are interesting in the distribution of two sides of the sheet along the ball surface and in the distribution of sheet fragments when the ball is cut in half. A hand folded paper ball is a very ill-defined system,

because the folding procedures appear quite haphazard and the number of possible folding configurations is exponentially large [24]. Nonetheless, experiments with hand folded paper are rather well reproducible in the statistical sense (see [3,4,9,15] and references therein), because of the topology and self-avoiding interactions are two most important physical factors when dealing with folding of thin materials [15,24].

The experiments in this work were performed with hand folded sheets of the *Biblia* paper of thickness $h=0.039\pm0.003$ early used in works [4,17,23]. We used square sheets with edge size $L=40$, 80, 160, 320, and 640 mm. 20 sheets of each size were folded in hands into approximately spherical balls. As it was found in [17], after the folding force is withdrawn, the ball diameter increases with time during approximately 6–9 days, due to the strain relaxation. Accordingly, in this work all measurements were performed two weeks after the folding, when no more changes in the ball dimensions were observed.

The mean diameter of each ball was determined from measurements along 15 directions taken at random. Than the surfaces of ten balls folded from sheets of each size were painted with paint brush [see Fig. 1(a)]. After unfolding, the both sides of each sheet were scanned with the resolution 200 ppp [see Fig. 1(b)–1(f)]. The rest ten balls of each size were cut in half [see Fig. 2(a)]. All fragments were weighted to obtain the fragment mass distribution. Then the sheet fragments from one ball half were painted in black, while the fragments from another half were lived in white. After this, the sheets were reconstructed, forming the black and white mosaic patterns [see Figs. 2(b)–2(f)].

The painted area on the each side of sheet we measured with use of scanned images [see Figs. 1(b)–1(f)]. These areas were labeled as S_A and S_B, such that per definition $S_A \geq S_B$. Figure 3(a) shows the graph of the sample averaged total area of folded ball $S=S_A+S_B$ versus its sample averaged diameter R together with the fractal graph $M \propto L^2$ versus R. One can see that the ball mass and the ball surface area both obey the fractal relation $M \propto R^D$ and $S \propto R^{D_S}$, respectively. We found that $D=2.27\pm0.05$ (see also [17]) and $D_S=2.11\pm0.05$ [see Fig. 3(a)], such that the scaling relationship $D_S=3-2/D$ (see [17]) is hold.

We also found that in balls folded from sheets of size $L<L_C$ one side of the sheet is dominant on the ball surface (see Fig. 1). As the sheet size increases the panted areas on both sides of sheet are increased in such a way that the ratio S_B/S_A decreases [see Figs. 1 and 3(a)]. The total painted area (unscreened perimeter) scales with the sheet size as $S=S_A+S_B \propto L^\gamma$ [see circles and solid line in Fig. 3(b)], where the scaling exponent $\gamma=2D_S/D$ is found to be $\gamma=1.85\pm0.08$. This is consistent with the values of D and D_S reported above. Besides we noted that the dependences of the sample averaged areas S_A and S_B can be also reasonably good fitted with the power-law relations $S_A=s_aL^\alpha$ and $S_B=s_bL^\beta$, respectively, at least within the bounded range of L tested in this work [see Fig. 3(b)].

Strictly speaking, the power-law behaviors $S_A=s_aL^\alpha$ and $S_B=s_bL^\beta$ are not consistent with the scaling relation $S=S_A+S_B \propto L^\gamma$. Nonetheless, the apparent scaling exponents $\alpha=1.69\pm0.08$ and $\beta=2.56\pm0.08$ provide a rough approxi-

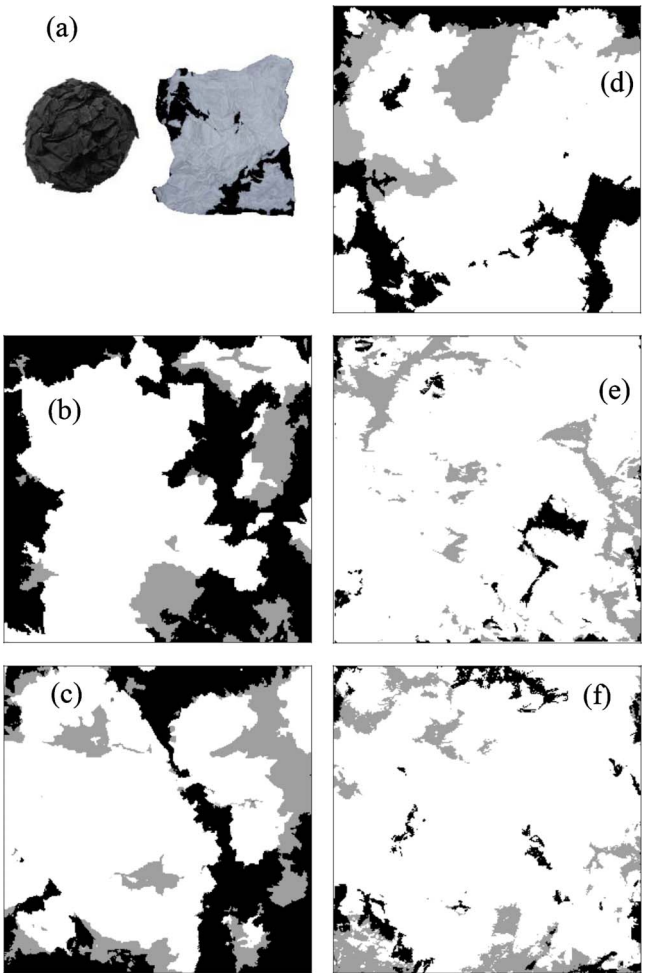

FIG. 1. (Color online) (a) Folded and unfolded ball of paper painted in black; (c)–(f) patterns obtained by mapping of ball surface into unfolded flat sheet of size: $L=40$ (b), 80 (c) 160 (d), 320 (e), and 640 mm (f). Back and gray areas correspond to ball surface mapping to different sides of paper sheet.

mates for the slopes of S_A and S_B for $L<L_C$ [see Fig. 3(b)]. So one may expect that in a ball folded from a sheet of size

$$L \geq L_C \approx (s_a/s_b)^{1/(\beta-\alpha)} \approx 1 \text{ m}, \tag{1}$$

the areas of both sides of the sheet along the ball surface will be statistically equal, i.e., $S_A \approx S_B \approx 0.5S(L \geq L_C)$. We noted that the ratio $h/L_C \approx 4\times10^{-5}$, such that the graphs in Fig. 3(b) suggest that two sides of folded sheet become statistically equivalent at very large Föppl–von Kármán numbers

$$\gamma=\left(\frac{YL^2}{\kappa}\right) \leq \gamma_C \approx \left(\frac{L_C}{h}\right)^2 \approx 10^9, \tag{2}$$

where Y is the two-dimensional Young's modulus of the sheet and κ is an effective bending modulus [10]. Notice that for the virus shells and nanocarbon sheets the Föppl–von Kármán number is in the range 10^2–10^4 [13] and so, the surfaces of these systems are expected to be dominated by one side of the folded matter. For macroscopic systems such

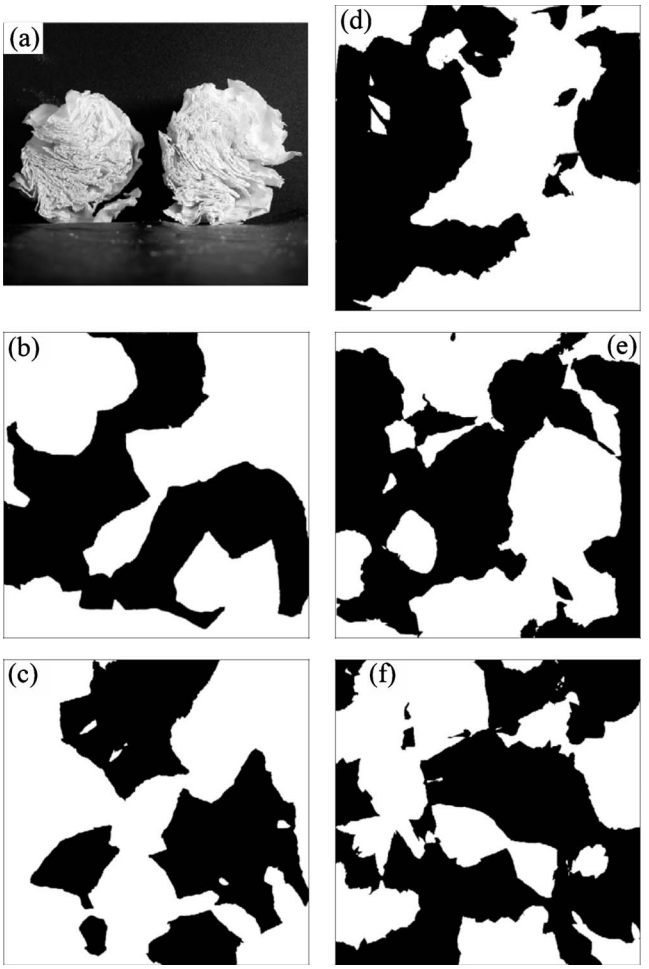

FIG. 2. (a) A ball of folded paper cut in half; (c)–(f) sheets of size $L=40$ (b), 80 (c) 160 (d), 320 (e), and 640 mm (f) reconstructed from fragments of paper ball divided in half (fragments from one part of the ball are painted in black).

as paper, mylar, and aluminum foils $10^5<\gamma<10^8$ [13] is also typically less than γ_C.

Furthermore, we found that the patterns obtained by mapping of ball surface into unfolded flat sheet exhibit the fractal properties characterized by two box fractal dimensions: $D_{BP}=1.8\pm0.1$ at small scales $\Delta<l_C$ and $D_{Bp}=1.42\pm0.06$ at larger scales $l_C<\Delta<L$ [see Fig. 4(a)], which are independent on L and R [see Fig. 4(b)]. The value of crossover length is varied from experiment to experiment in the range of $1.5\leq l_C\leq 4$ mm with no systematic dependence on the sheet size [see Fig. 4(b)]. Accordingly, the ratio l_C/h is of the order of 100. While the scaling behavior at low scales may be interpreted as an artifact, we assume the crossover behavior of painted patterns, because the slope of the low scale behavior $N(\Delta\leq l_C)\propto\Delta^{D_{BP}}$ is found to be the same in all experiments. However, the reason for the crossover at $\Delta=l_C$ is unclear.

Further, we found that the number of fragments of paper ball cut in half scales with the sheet size as $n\propto L^{\nu}$, where the scaling exponent is found to be $\nu=0.26\pm0.03$ [see Fig. 5(a)], while the standard deviation of the number of

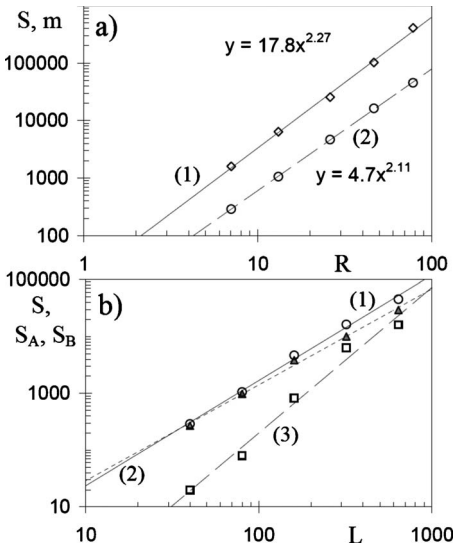

FIG. 3. Log-log plots of: (a) the total area of folded ball surface S in mm^2 (1) and the normalized ball mass $m=M/h\rho=L^2$ in mm^2 (2) versus R in mm; (b) the total area of folded ball surface S in mm^2 (1) and the panted areas on two sides of unfolded sheet S_A in mm^2 (2) and S_B in mm^2 (3) versus sheet size L (in cm). Symbols—experimental data averaged over ten sheets, lines—the power-law fittings.

fragments scales as $\sigma_n\propto L^{0.3}$ [see Fig. 5(b)]. The distribution of sheet fragment mass after the ball is cut in half is best fitted with inverse Gaussian distribution [see Fig. 6(a)], the mean μ and the standard deviation σ_μ of which [see Fig. 6(b)] both increase with the sheet size L as

$$\mu\propto\sigma_\mu\propto L^{\theta} \tag{3}$$

where $\theta=1.74\pm0.07$ is the scaling exponent [see Figs. 7(a) and 7(b)]. Accordingly, the mean mass of fragments from hand folded balls of paper cut in half obeys the scaling relation $\mu\propto R^{D\theta/2}\propto R^2$.

Besides, we found that the mosaic patterns of sheet fragments [see Figs. 2(b)–2(f)] possess a fractal scale invariance characterized by the box fractal dimension

$$D_{BF}=1.68\pm0.04, \tag{4}$$

which is found to be independent on the sheet size (see Fig. 8). We noted that the fractal dimension D_{BF} at least numerically coincides with the fractal dimension of the intersection of hand folded paper ball with a plane, $D_{BI}=D_l-1=1.64\pm0.05$ [4]. The later is expected to be universal, since the experimental data suggest that the local fractal dimension of paper ball after strain relaxation is independent on the kind of paper, sheet size and thickness, and the initial compression ratio [25]. Moreover, early [4], it was noted that the experimental value of D_l coincides with the universal mass fractal dimension $D=8/3$ of a set of phantom sheets of different sizes folded under the same force ($F=$const). So, if the equality

$$D_{BF}=D_{BI} \tag{5}$$

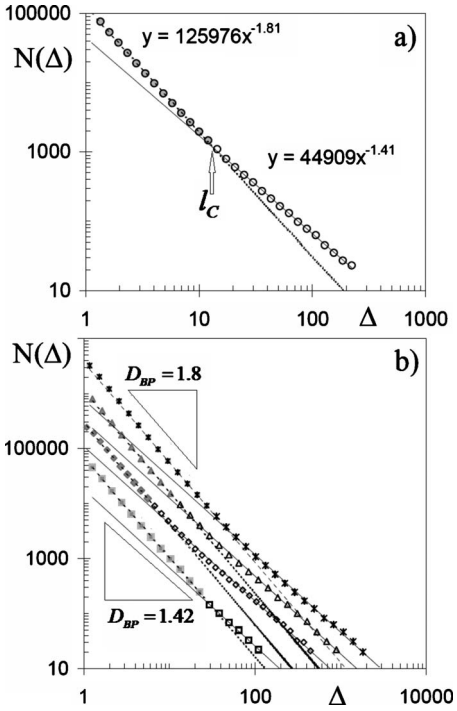

FIG. 4. The fractal log-log plots of the number of boxes $N(\Delta)$ covering the black patterns in unfolded sheets of size (a) $L=80$ mm (circles), (b) $L=40$ (squares), 160 (rhombs), 320 (triangles), and 640 mm (crosses) versus the box size Δ (in pixels). Symbols—experimental data obtained with the help of the BENOIT 1.3 software [26] averaged over ten sheets (to avoid the effect of pattern anisotropy the grids were rotated with increments of 15°), lines–the power-law fittings.

is not accidental, the fractal dimension D_{BF} is also expected to be universal. It should be pointed out that the universality of fractal dimensions D_{BI} and D_{BF} is not in the conflict with the experimental fact that the global mass fractal dimension D is the material dependent. In fact, D characterizes the scaling properties of the set of balls folded from sheets of different sizes, whereas D_{BI} and D_{BF} characterize the scaling properties of the internal configuration of folded sheet.

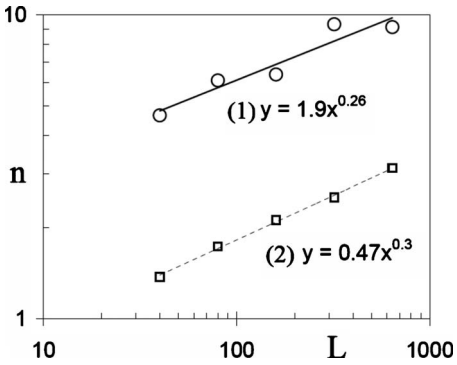

FIG. 5. Log-log plots of the mean number n (1) and the standard deviation σ_n (2) of fragments of paper balls cut in half versus the sheet size L in mm. Symbols—experimental data, lines—the power-law fittings.

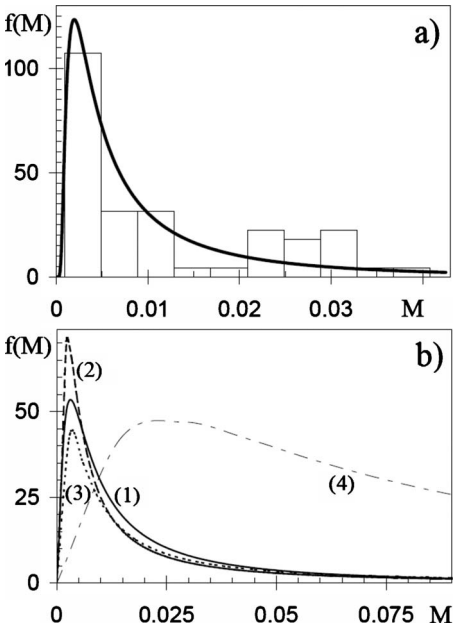

FIG. 6. Statistical distributions of the mass of fragments of 10 balls folded cut in half for balls folded from square sheets of edge size (a) $L=40$ mm (bins—experimental data, solid line—fitting with the Gamma distribution with the help of @RISK software [27], p-value is 0.41) and (b) $L=80$ (1) 160 (2), 320 (3), and 640 mm (4) (the bins are not shown for clarity).

In summary, we present the results of experimental studies statistical topology of folding configurations of hand folded paper balls. Some new fractal properties of folding configurations are recognized. Specifically, we found that in a ball folded from paper sheet of size $L<L_C$ one side of the sheet is dominant on the ball surface, whereas in a ball folded from paper sheet of size $L>L_C$, the areas of both

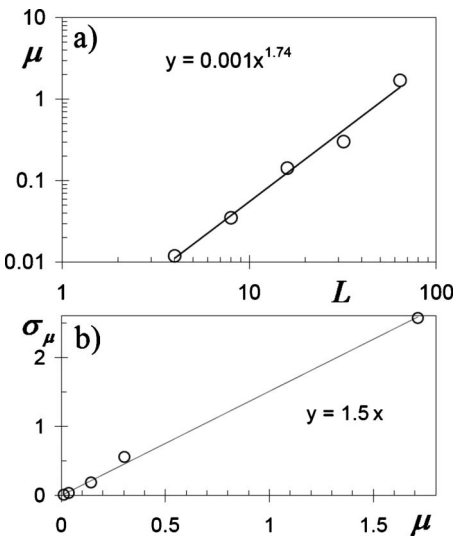

FIG. 7. (a) Log-log plot of the mean mass M (in grams) of fragments versus sheet size L (in mm); (b) graph of the standard deviation fragment mass σ_μ (in grams) versus the mean fragment mass μ (in grams). Symbols—experimental data averaged over ten sheets, lines—the power-law fittings.

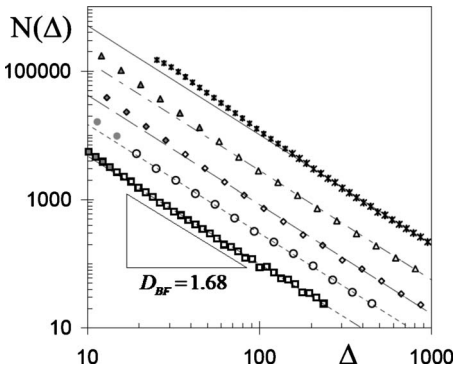

FIG. 8. The fractal log-log plots of the number of boxes $N(\Delta)$ covering the black (white) patterns in reconstructed sheets of size $L=40$ (squares), 80 (circles), 160 (rhombs), 320 (triangles), and 640 mm (crosses) versus the box size Δ (in pixels). Symbols—experimental data obtained with the help of the BENOIT 1.3 software [26] averaged over 20 patterns from 10 reconstructed sheets (to avoid the effect of pattern anisotropy the grids were rotated with increments of 15°), lines—the power-law fittings (gray symbols are excluded from the fitting).

sheet sides along the ball surface are statistically equal. In a set of balls folded from sheets of different sizes, the total area of the ball scales with the ball diameter as $S \propto R^{D_S}$ with the fractal dimension D_S satisfying the scaling relation $D_S=3-2/D$, where D is the mass fractal dimension of the set of balls. The patterns obtained by mapping of ball surface into unfolded flat sheet exhibit the fractal properties characterized by two fractal dimensions, which are independent on L and R.

We also found that the distribution of sheet fragment mass after the ball is cut in half obeys inverse Gaussian distribution, the mean and the standard deviation of which are power-law functions of the sheet size L. The mosaic patterns obtained by sheet reconstruction from fragments of two parts of the ball cut in half possess a fractal scale invariance characterized by the box fractal dimension $D_{BF}=1.68\pm0.04$, which, at least numerically, coincide with the universal fractal dimension of the intersection of hand folded paper ball with a plane. If this coincidence is not accidental, fractal dimension D_{BF} is expected to be universal. In any case, we found that D_{BF} is independent on the sheet size.

These findings provide an insight into the nature of crumpling phenomena. The open questions are: (i) What is the reason for the crossover in the scaling properties of unscreened surface of folded sheet? (ii) Is the equality $D_{BF}=D_{BI}=D_l-1=5/3$ accidental, or it is an intrinsic property of folding configurations? We are expecting that our findings will stimulate further research in this area.

This work was supported by the Government of Mexico City under Project PICCT08-38.

[1] B. Honig, J. Mol. Biol. **293**, 283 (1999); A. V. Finkelstein and O. V. Galzitskaya, Phys. Life. Rev. **1**, 23 (2004); E. Tejera, A. Machado, I. Rebelo, and J. Nieto-Villar, Physica A **388**, 4600 (2009).

[2] T. Hwa, E. Kokufuta, and T. Tanaka, Phys. Rev. A **44**, R2235 (1991); M. S. Spector, E. Naranjo, S. Chiruvolu, and J. A. Zasadzinski, Phys. Rev. Lett. **73**, 2867 (1994); Y. Lin, H. Skaff, A. Böker, D. A. Dinsmore, T. Emrick, and T. P. Russell, J. Am. Chem. Soc. **125**, 12690 (2003); Q. Kuang, S.-Y. Xie, Zh.-Y. Jiang, S. H. Zhang, Zh.-X. Xie, R. B. Huang, and L. S. Zheng, Carbon **42**, 1737 (2004).

[3] D. L. Blair and A. Kudrolli, Phys. Rev. Lett. **94**, 166107 (2005); E. Sultan and A. Boudaoud, *ibid.* **96**, 136103 (2006); J. Guven and M. M. Müller, J. Phys. A: Math. Theor. **41**, 055203 (2008).

[4] A. S. Balankin, R. C. Montes de Oca, and D. Samayoa, Phys. Rev. E **76**, 032101 (2007).

[5] D. M. Hansen and J. Cartwright, J. Struct. Geol. **28**, 1520 (2006); Z. Ismat, *ibid.* **31**, 972 (2009).

[6] M. Kaku, *Hyperspace: A Scientific Odyssey through Parallel Universes, Time Warps, and the* 10^{th} Dimension (Oxford University Press, New York, 1994).

[7] P. Di Francesco, Bull. Am. Math. Soc. **37**, 251 (2000); E. D. Demaine, Lect. Notes Comput. Sci. **2098**, 113 (2001); T. Biedl, A. Lubiw, and J. Sun, Comput. Geom. **31**, 207 (2005).

[8] R. Lipowsky, Nature (London) **349**, 475 (1991); G. Gompper, *ibid.* **386**, 439 (1997); E. Cerda, S. Chaieb, F. Melo, and L. Mahadevan, *ibid.* **401**, 46 (1999); A. Boudaoud, P. Patrício, Y. Couder, and M. Ben Amar, *ibid.* **407**, 718 (2000); R. Lakes, *ibid.* **414**, 503 (2001); M. J. Bowick and A. Travesset, Phys. Rep. **344**, 255 (2001); B. Didonna, Nature Mater. **5**, 167 (2006); M. Marder, R. D. Deegan, and E. Sharon, Phys. Today **60**(2), 33 (2007); Y. Klein, E. Efrati, and E. Sharon, Science **315**, 1116 (2007).

[9] M. A. F. Gomes, T. I. Lih, and T. I. Ren, J. Phys. A **23**, L1281 (1990); J. B. C. García, M. A. F. Gomes, T. I. Jyh, and T. I. Ren, *ibid.* **25**, L353 (1992); M. A. F. Gomes, T. I. Lih, and T. I. Ren, J. Phys. D **40**, 3665 (2007); C. C. Donato and M. A. F. Gomes, Phys. Rev. E **75**, 066113 (2007).

[10] A. E. Lobkovsky, Sh. Gentges, H. Li, D. Morse, and T. A. Witten, Science **270**, 1482 (1995); A. E. Lobkovsky, Phys. Rev. E **53**, 3750 (1996); E. M. Kramer and A. E. Lobkovsky, *ibid.* **53**, 1465 (1996); P. A. Houle and J. P. Sethna, *ibid.* **54**, 278 (1996); E. M. Kramer and T. A. Witten, Phys. Rev. Lett. **78**, 1303 (1997); E. Cerda and L. Mahadevan, *ibid.* **80**, 2358 (1998); B. A. DiDonna and T. A. Witten, *ibid.* **87**, 206105 (2001); K. Matan, R. B. Williams, T. A. Witten, and S. R. Nagel, *ibid.* **88**, 076101 (2002); A. Gopinathan, T. A. Witten, and S. C. Venkataramani, Phys. Rev. E **65**, 036613 (2002); B. A. DiDonna, *ibid.* **66**, 016601 (2002); J. A. Aström, J. Timonen, and M. Karttunen, Phys. Rev. Lett. **93**, 244301 (2004); T. Liang and T. A. Witten, Phys. Rev. E **71**, 016612 (2005); A. S. Balankin, *et al.*, *ibid.* **73**, 065105(R) (2006); N. Stoop, F. K. Wittel, and H. J. Herrmann, Phys. Rev. Lett. **101**, 094101 (2008); T. Tallinen, J. A. Aström, and J. Timonen, *ibid.* **101**, 106101 (2008); A. S. Balankin and O. Susarrey Huerta, Phys.

Rev. E **77**, 051124 (2008); O. Susarrey Huerta, M. Mendoza Nuñez, P. A. Tamayo Meza, and A. S. Balankin, Adv. Mater. Res. **65**, 33 (2009); S. Deboeuf, M. Adda-Bedia, and A. Boudaoud, EPL **85**, 24002 (2009); T. A. Witten, J. Phys. Chem. B **113**, 3738 (2009).

[11] T. A. Witten, Rev. Mod. Phys. **79**, 643 (2007).

[12] M. A. F. Gomes, Am. J. Phys. **55**, 649 (1987); J. Phys. A **20**, L283 (1987); R. Cassia-Moura and M. A. F. Gomes, J. Theor. Biol. **238**, 331 (2006).

[13] G. A. Vliegenthart and G. Gompper, Nature Mater. **5**, 216 (2006).

[14] T. Tallinen, J. A. Aström, and J. Timonen, Nature Mater. **8**, 25 (2009).

[15] A. S. Balankin, D. Morales, E. Pineda León, A. Horta Rangel, M. A. Martínez Cruz, and D. Samayoa, Physica A **388**, 1780 (2009).

[16] It should be pointed out that that $D=2.3$ was calculated in [13] using the scaling relationship between D and the scaling exponents governing the force-compression relation, while in [14] the fractal dimension $D=2.5$ was obtained from direct numerical simulations.

[17] A. S. Balankin, O. Susarrey, R. C. Montes de Oca, D. Samayoa, J. Martinez Trinidad, and M. Mendoza, Phys. Rev. E **74**, 061602 (2006).

[18] R. F. Albuquerque and M. A. F. Gomes, Physica A **310**, 377 (2002); A. S. Balankin, I. Campos Silva, O. A. Martinez, and O. Susarrey, Phys. Rev. E **75**, 051117 (2007); Y. C. Lin, Y. L. Wang, Y. Liu, and T. M. Hong, Phys. Rev. Lett. **101**, 125504 (2008).

[19] Y. C. Lin, J. M. Sun, H. W. Yang, C. L. Wang, Y. Hwu, and T. M. Hong, Phys. Rev. E **80**, 066114 (2009).

[20] Y. C. Lin, J. M. Sun, J. H. Hsiao, Y. Hwu, C. L. Wang, and T. M. Hong, Phys. Rev. Lett. **103**, 263902 (2009).

[21] S. C. Venkataramani, T. A. Witten, E. M. Kramer, and R. P. Geroch, J. Math. Phys. **41**, 5107 (2000).

[22] Ch. A. Andresen and A. Hansen, Phys. Rev. E **76**, 026108 (2007).

[23] A. S. Balankin and O. Susarrey, in *Proceedings of IUTAM Symposium on Scaling in Solid Mechanics*, edited by F. Borodich (Springer, Cardiff, 2009).

[24] Y. Kantor, M. Kardar, and D. R. Ne1son, Phys. Rev. A **35**, 3056 (1987).

[25] The strain relaxation after the folding force is withdrawn is essential for the universality of local fractal dimension D_l, since under increasing folding force D_l will increase up to $D_l=3$, when the folded ball becomes compact without porosity. Notice that the porosity of all paper balls used in this work was larger than 80%.

[26] BENOIT 1.3, http://www.trusoft-international.com; W. Seffens, Science **285**, 1228 (1999).

[27] The goodness-of-fit tests with the Chi-squared, Kolmogorov-Smirnov, and Anderson statistics were performed with the help of @RISK software (http://www.palisade.com).